Neoplasia • Vol. 9, No. 12, December 2007, pp. 1138–1151

www.neoplasia.com

Hypoxia and the Presence of Human Vascular Endothelial Cells Affect Prostate Cancer Cell Invasion and Metabolism[1]

Ellen Ackerstaff[*,†,2], *Dmitri Artemov*[*,†], *Robert J. Gillies*[‡] *and Zaver M. Bhujwalla*[*,†]

*Russell H. Morgan Department of Radiology and Radiological Science, Johns Hopkins University School of Medicine, 720 Rutland Ave., Traylor Bldg. 217, Baltimore, MD 21205, USA; †Department of Oncology, Johns Hopkins University School of Medicine, 720 Rutland Ave., Traylor Bldg. 217, Baltimore, MD 21205, USA; ‡Department of Biochemistry and Molecular Biophysics, Arizona Cancer Center, University of Arizona, 1515 N. Campbell #0985, Tucson, AZ 85724, USA

Abstract

Tumor progression and metastasis are influenced by hypoxia, as well as by interactions between cancer cells and components of the stroma, such as endothelial cells. Here, we have used a magnetic resonance (MR)–compatible invasion assay to further understand the effects of hypoxia on human prostate cancer cell invasion and metabolism in the presence and absence of human umbilical vein endothelial cells (HUVECs). Additionally, we compared endogenous activities of selected proteases related to invasion in PC-3 cells and HUVECs, profiled gene expression of PC-3 cells by microarray, and evaluated cell proliferation of PC-3 cells and HUVECs by flow cytometry, under hypoxic and oxygenated conditions. The invasion of less-invasive DU-145 cells was not affected by either hypoxia or the presence of HUVECs. However, hypoxia significantly decreased the invasion of PC-3 cells. This hypoxia-induced decrease was attenuated by the presence of HUVECs, whereas under oxygenated conditions, HUVECs did not alter the invasion of PC-3 cells. Cell metabolism changed distinctly with hypoxia and invasion. The endogenous activity of selected extracellular proteases, although altered by hypoxia, did not fully explain the hypoxia-induced changes in invasion. Gene expression profiling indicated that hypoxia affects multiple cellular functions and pathways.

Neoplasia (2007) **9,** 1138–1151

Keywords: Prostate cancer, hypoxia, invasion, endothelial/cancer cell interaction, magnetic resonance (MR) imaging and spectroscopy.

Introduction

Tumor progression and metastasis can be influenced by the microenvironments within a solid tumor, as well as by interactions between cancer cells and components of the stroma, such as endothelial cells [1,2]. Areas of hypoxia, extracellular acidosis, and substrate deprivation frequently characterize the tumor microenvironment [3,4]. Low oxygen tensions (< 10 mm Hg) in the primary tumor have been associated with increased incidence of metastases in carcinoma of the cervix, head, and neck, as well as in soft tissue sarcoma [3]. The endothelial cell lining of tumor blood vessels, and endothelial cell injury, which may occur with hypoxia, can also play an important role in cancer invasion and metastasis [1,2].

Tumor hypoxia can alter the activities of membrane-bound or -secreted proteinases, such as matrix metalloproteinase 2 (MMP-2), 9 (MMP-9), and urokinase-type plasminogen activator (uPA), which play a critical role in extracellular matrix (ECM) remodeling and cancer cell invasion [5,6]. Cancer cells express and secrete proteolytic enzymes. However, most proteolytic components are produced by stromal cells, such as endothelial cells, responding to tumor cells [5]. With the exception of MMP-11 and membrane type 1–MMP, proteases are expressed extracellularly as inactive proforms that become activated through a variety of mechanisms that often involve a close collaboration among several families of proteases [7]. MMPs seem to play a critical role in the proteolytic modification of ECM proteins, such as laminin 5 and fibrillar collagen, and in increasing the solubility of some angiogenic factors, such as vascular endothelial growth factor (VEGF), but can also target non–ECM proteins [7]. The activation of proteolysis by the plasminogen activator system has been reported in several human malignancies and is believed to contribute to tumor cell motility and invasion [8]. Specifically, MMP-2, MMP-9, and uPA have been related to the

Abbreviations: CSI, chemical shift imaging; [d], [days]; ECM, extracellular matrix; EGM, endothelial growth medium; FBS, fetal bovine serum; GPC, glycerophosphocholine; HIF, hypoxia-inducible factor; HUVECs, human umbilical vein endothelial cells; Lac, lactate; LacTG, lactate + triglycerides; MMP, matrix metalloproteinase; MBC, Metabolic Boyden Chamber; MR, magnetic resonance; PC-3_{Bb}, PC-3 on Biosilon beads; PC, phosphocholine; $RPMI_c$, RPMI 1640 supplemented with 9% FBS, 90 U/ml penicillin, and 90 μg/ml streptomycin; tCho, total choline (choline + phosphocholine + glycerophosphocholine); tCr, total creatine (creatine + phosphocreatine); TG, triglycerides; uPA, urokinase-type plasminogen activator; VEGF, vascular endothelial growth factor

Address all correspondence to: Dr. Zaver M. Bhujwalla, Russell H. Morgan Department of Radiology, Johns Hopkins University School of Medicine, 720 Rutland Ave., 208C Traylor Bldg., Baltimore, MD 21205. E-mail: zaver@mri.jhu.edu

[1]This work was supported by a National Institutes of Health grant (2RO1 CA73850). This article refers to supplementary materials, which are designated by Tables W1 and W2 and Figure W1 and are available online at www.neoplasia.com.

[2]Current address: Memorial Sloan-Kettering Cancer Center, 1275 York Ave., New York, NY 10021, USA.

Received 8 July 2007; Revised 12 October 2007; Accepted 15 October 2007.

DOI 10.1593/neo.07568

invasive capacity of cancer cells and proposed as molecular markers of invasion (e.g., [8,9]). Additionally, growth factors and cytokines can modulate proteolytic enzyme expression and activity [1]. Also, hypoxia increases the transcription of hypoxia-induced target genes but may also result in specific gene repression [10].

The invasive potential of cancer cells is commonly assayed by determining the penetration of cells into reconstituted basement membrane gel or ECM gel. Invasion is quantified by counting the number of cells that invade through ECM gel–coated filters within a specific time interval [11]. This method cannot dynamically measure the invasion and metabolism of cancer cells in the same sample under controlled environmental conditions, or following interventions. To overcome some of these limitations, we used a previously described magnetic resonance (MR)–compatible invasion assay to dynamically track and quantify the invasion of cancer cells over time, and simultaneously characterize oxygen tensions, as well as physiology and metabolism [12–14].

In this study, we determined the effects of hypoxia on prostate cancer cell invasion and metabolism and investigated the contribution of endothelial cells to the invasive process under oxygenated and hypoxic conditions by inserting a layer of human umbilical vein endothelial cells (HUVECs) between the ECM gel layer and the cancer cells. Although human tumor–derived endothelial cells would be the most relevant cells to use, these are difficult to isolate and culture, whereas HUVECs provided a stable source of endothelial cells. Because MMP-2, MMP-9, and uPA have been proposed as biomarkers of invasion (e.g., [8,9]), we focused on evaluating the endogenous activities of these proteolytic enzymes in PC-3 cells and HUVECs under oxygenated and hypoxic conditions. We also obtained gene expression profiles of oxygenated and hypoxic PC-3 cells by microarray analysis to discern patterns associated with cancer cell invasion and metabolism. Cell proliferation under both conditions was evaluated to understand its role in the changes in invasion observed here. Our results demonstrate that hypoxia did not increase the invasiveness of the malignant epithelial cells studied, but that endothelial cells facilitated invasion under hypoxic conditions. These results also demonstrate that functional assays are critical in determining the ultimate effect of microenvironmental changes on cancer cell invasion, because studying changes in gene or protease expression may not directly reflect the endpoint.

Materials and Methods

Cell Lines and Cell Culture

Experiments were performed using two human prostate cancer cell lines PC-3 (American Type Culture Collection, Manassas, VA) and DU-145 (kindly provided by Dr. J. Nelson, University of Pittsburgh, Pittsburgh, PA) [15]. PC-3 cells were cultured in $RPMI_c$, i.e., RPMI 1640 (Sigma, St. Louis, MO) supplemented with 9% fetal bovine serum (FBS; Sigma), 90 U/ml penicillin (Invitrogen Corp., Grand Island, NY), and 90 μg/ml streptomycin (Invitrogen Corp.). DU-145 cells were cultured in minimum essential medium (Cellgro; Mediatech Inc., Herndon, VA), containing Earle's salt and L-glutamine, supplemented with 9% FBS, 90 U/ml penicillin, and 90 μg/ml streptomycin. Human umbilical vein endothelial cells, obtained from Clonetics (Walkersville, MD), were cultured in medium provided in the endothelial growth medium 2 (EGM-2) Bulletkit (Clonetics). All cells were maintained at 37°C, 5% CO_2 in air, and 90% humidity. The pH of the cell culture media was 7.2 ± 0.2.

Cell Culture for MR Experiments

Before each MR experiment, 3×10^6 PC-3 cells or 1.5×10^6 DU-145 cells were seeded on 0.5 ml of Biosilon beads (Nunc, Denmark) in 100-mm bacteriological Petri dishes (Labtek, Nunc, Denmark) containing 15 ml of cell culture medium, which was changed daily. Cells reached approximately 90% confluence on the surface of the beads within 3 days for PC-3 cells and 4 days for DU-145 cells (Figure 1*A*). Cells on beads were counted at the beginning and at the end of each experiment as described previously [13,14]. For MR experiments investigating endothelial/cancer cell interaction, 5×10^4 HUVECs were seeded on ECM gel (from Engelbreth-Holm-Swarm murine sarcoma, diluted to 8.8 mg protein/ml; Sigma) contained in a home-built chamber, approximately 15 hours before the MR experiment. This time interval allowed endothelial cells to attach to the ECM gel and form a branching tubular network (Figure 1*A*) previously reported in other studies [16,17]. Tubular network formation by HUVECs on ECM gel was completed within 18 hours, stable up to 3 days, and accompanied by loss of detectable cell proliferation [17].

The Metabolic Boyden Chamber

A schematic of the sample structure is shown in Figure 1*A* and a detailed description of the MR cell perfusion system can be found in the works of Pilatus et al. [13] and Ackerstaff et al. [14]. Briefly, adherently grown cancer cells were layered around an ECM gel chamber. Two layers of perfluorocarbon-doped alginate beads were interspersed within the layers of cancer cells grown on Biosilon beads to monitor the oxygen tension in the sample using ^{19}F MR relaxometry (Figure 1, *A* and *B*) [13,18]. In some experiments, perfluorocarbon was added to the ECM gel to obtain oxygen tension within the ECM layer. The oxygen tension in the sample was kept at $[O_2] \geq 20\%$ during control experiments, and adjusted to $[O_2] \leq (1.0 \pm 0.5)\%$ in experiments studying the effects of hypoxia on the invasion and metabolism of cancer cells (Figure 1*B*) [18]. The sample was perfused continuously with cell culture medium supplemented with 10 mM Hepes (Sigma) at a flow rate of approximately 1 ml/min. The temperature was maintained at 37°C and the pH at 7.30 ± 0.15 for all MR experiments.

Because human CD31 antigen is constitutively expressed on the surface of endothelial but not epithelial cells [19], the presence of HUVECs at the end of the MR experiment was confirmed by immunofluorescent staining with a fluorescent anti–CD31 mouse monoclonal antibody [CD31/PECAM-1 Ab-5 (clone HC1/6); Neomarkers Inc., Fremont, CA], as shown in Figure 1*C*.

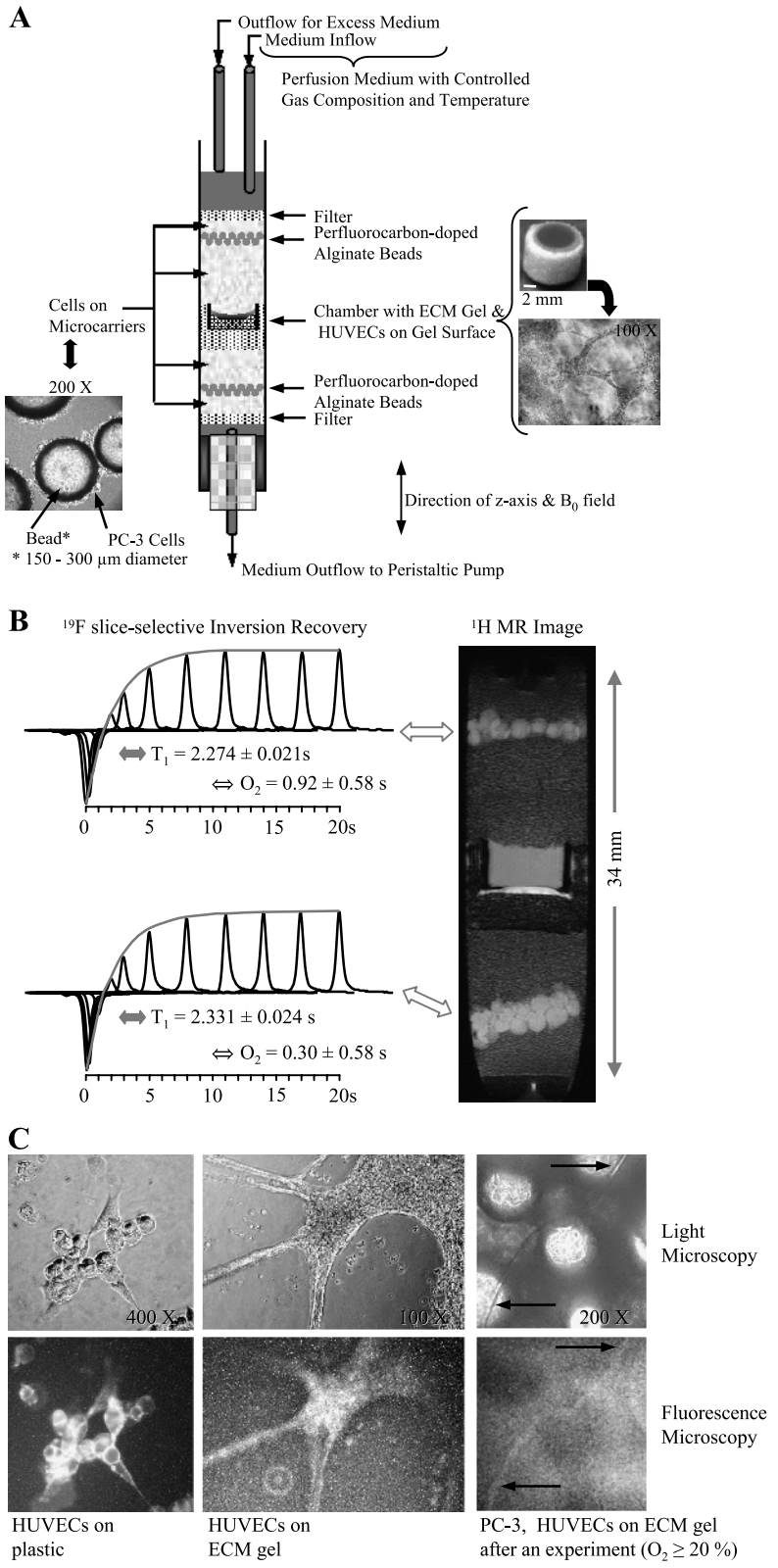

Figure 1. *(A) Photomicrograph of PC-3 cells grown adherently on microcarriers (left) and schematic display of the sample structure (center). On the right are photomicrographs of the invasion chamber filled with ECM gel (top) and an example of the distribution of HUVECs on the ECM gel at the start of an experiment (bottom). (B) Oxygen tension measurement in the MBC. Reprinted with permission from Pathak et al. [18]. (C, left to right) Representative phase contrast light micrographs (upper panel) and wide-field fluorescence images (lower panel) obtained after fluorescent anti–CD31 mouse monoclonal antibody staining of HUVECs on tissue culture plastic (1:50 dilution) (left), on ECM gel (1:50 dilution) (center), and at the end of an MR experiment (1:10 dilution, 20-minute incubation time) (right). The control experiments revealed specific staining of HUVECs (C, left), but neither the PC-3 cells (data not shown) nor the ECM gel was stained (C, center). Despite the higher background fluorescence due to the autofluorescence of Biosilon beads, a capillary-like structure staining positively for CD31 was identified in images taken at the end of a 3-day experiment with the MBC (C, right, arrows), confirming the presence of viable HUVECs. Wide-field fluorescence and corresponding phase contrast micrographs were captured on an inverted microscope (ECLIPSE TS100) equipped with a digital camera (Coolpix 990; Nikon Corporation, Tokyo, Japan). An excitation bandwidth of 450 to 490 nm and an emission bandwidth of 500 to 550 nm were used for fluorescence imaging.*

MR Data Acquisition, Processing, and Analysis

The MR data acquisition, processing, and analysis have been described in detail in the study of Ackerstaff et al. [14]. Briefly, the following series of MR acquisitions were acquired on a 9.4 T MR spectrometer (Omega, GE/Bruker, Billerica, MA) every 12 hours throughout the experiment. Proton MR imaging was performed to evaluate the sample preparation, to visualize the geometry of the ECM gel, and to detect changes in the integrity of the ECM gel due to invasion and degradation by cancer cells. One-dimensional (1D) ^{1}H MR profiles of intracellular water were acquired along the length of the sample to obtain an invasion index. Energy metabolites, pH, and the choline phospholipid metabolites, phosphocholine (PC) and glycerophosphocholine (GPC), were obtained from global 1D ^{31}P MR spectra. Intracellular levels of total choline (tCho, signals from PC + GPC + free choline), total creatine (tCr, signals from creatine + phosphocreatine (PCr)), and lactate/triglycerides (LacTG) were derived from global, diffusion-weighted (DW) 1D ^{1}H MR spectra. Diffusion-weighted 1D ^{1}H MR spectra, obtained without water suppression, were used to determine cell proliferation, because the increase of slow-diffusing water, which represents intracellular water, was directly proportional to the number of cells. Because the degradation of ECM by cells also depends on the number of cells, it was necessary to normalize the invasion index to the proliferation of cells that occurred over the 2- to 3-day period used in our studies. Additionally, DW 1D ^{1}H MR spectra were acquired using Lac editing to quantify the contribution of Lac and TG to the LacTG signal.

Localized DW 1D ^{1}H chemical shift imaging (CSI) spectra with and without water suppression were acquired to obtain metabolic information from 310-μm-thick slices along the *z*-axis of the sample. The oxygen tension was obtained from slice-selective 1D ^{19}F inversion recovery MR experiments. Localized 1D ^{1}H CSI and ^{19}F MR spectra were acquired every 24 hours.

Values, presented as mean ± SE, were averaged over four independent experiments ($n = 4$) for each condition, unless otherwise stated. Statistically significant differences ($P < .05$) for the different conditions were evaluated by the Mann-Whitney U test unless otherwise stated.

Cell Cycle Analysis

Cell cycle analysis was performed using a fluorescein isothiocyanate bromodeoxyuridine flow kit (BD Biosciences Pharmingen, San Diego, CA).

PC-3 cells were seeded at a cell density of 4×10^4 cells/cm^2 in tissue culture flasks and allowed to attach overnight. Freshly thawed HUVECs were allowed to recover for 2 to 3 days. Following the replacement of the culture medium with fresh RPMI$_c$, the PC-3 cells and the 10-day-old HUVECs were placed for 48 hours at 37°C and 90% humidity either in a tissue culture incubator with 20% O_2 and 5% CO_2 or in a hypoxia chamber (BioSpherix Ltd., Redfield, NY) set to 1% O_2 and 5% CO_2. After 48 hours, the conditioned media were collected, aliquoted, and stored at −80°C until enzymatic analysis. At the same time, the cells were incubated for 100 minutes or 154 minutes with bromodeoxyuridine labeling solution, then harvested and prepared for flow cytometry following the manufacturer's protocol, including the optional step of staining for total DNA using 7-amino actinomycin D. Two-color flow cytometric analysis was performed to enumerate cells that actively synthesized DNA, using a FACScalibur flow cytometer (Becton Dickinson, San Jose, CA) equipped with lasers exciting at 488 nm and 633 nm. Three independent experiments were performed. Significant differences were tested by two-way analysis of variance without interaction using the condition and cell batch as nominal classification variables and the percentage of cells as the response variable.

Enzyme Activity Assays

MMP-2, MMP-9, and uPA protease activities were determined in conditioned media of PC-3 cells and HUVECs in tissue culture obtained and stored as described in the Cell Cycle Analysis section, as well as in conditioned media of samples that mimicked the cellular conditions in the Metabolic Boyden Chamber (MBC) experiments. For the latter, six ECM gel inserts were prepared by polymerizing 200 μl ECM gel (8.8 mg protein/ml) per insert (Isopore track–etched polycarbonate, 0.4 μm pore size; Millipore, Bedford, MA) in a six-well tissue culture plate. Into each of four of these ECM gel inserts, 1.1×10^5 HUVECs in EGM-2 were plated and the inserts placed overnight in EGM-2 to allow for attachment and network formation. Approximately 0.4 ml PC-3 cells grown on Biosilon beads (PC-3$_{Bb}$), as described in the Cell Culture for MR Experiments section, were added to each of two ECM gel inserts and of two ECM gel inserts containing HUVECs. The inserts were divided into the following two groups subjected to either 20% O_2 or 1 ± 0.2% O_2 for 48 hours as described in the Cell Cycle Analysis section: 1) PC-3$_{Bb}$ on ECM gel, 2) PC-3$_{Bb}$ and HUVECs on ECM gel, and 3) HUVECs on ECM gel. All inserts were placed in 10 ml RPMI$_c$. After 48 hours, PC-3$_{Bb}$ were counted as described previously, and the conditioned media were collected, aliquoted, and stored at −80°C until enzymatic analysis.

The endogenous enzymatic activities of MMP-2 and MMP-9 were determined from two independent experiments using the human MMP-2 and MMP-9 Biotrak Activity Assay[3] (GE Healthcare, formerly Amersham Biosciences, Piscataway, NJ) respectively, and uPA from one experiment using the Chemicon uPA Activity Assay Kit (Chemicon, Temecula, CA).

Isolation of Total RNA and Human Genome Array

Following attachment overnight and replacement of RPMI$_c$, PC-3 cells (3.8×10^4 cells/cm^2 seeding density) were exposed to 20% or 1% oxygen for 48 hours.

Total cellular RNA of PC-3 cells was isolated using QIAshredder homogenizer spin columns (Quiagen Inc., Valencia, CA) and the RNeasy Mini Kit (Quiagen Inc.), including DNase digestion. The RNA was quantified and evaluated for purity.

[3]Variability in absolute quantification of MMP-2 and MMP-9 activities was introduced by the deterioration of standards with storage. The enzyme activities were higher in the second experiment. However, as the results within an experiment were reproducible, comparison between the different conditions was possible.

The RNA labeling, microarray hybridization, and quality control were performed as described in detail elsewhere [14] by the Johns Hopkins Medical Institutions Microarray Core facility (Dr. F.M. Murillo, Johns Hopkins University, Baltimore, MD). Two independent experiments each were run for oxygenated and hypoxic PC-3 cells.

The analysis of the human genome array data was performed at the Analysis Unit of the Johns Hopkins Medical Institutions Microarray Core (Dr. Chunfa C. Jie, Johns Hopkins University, Baltimore, MD) and has been described previously in detail [14]. The gene annotations corresponding to Affymetrix probe names are current as of June 2005. The list of genes that were differentially expressed between hypoxic and oxygenated PC-3 cells was produced by applying a posterior probability above 0.5; that is, the posterior probability is larger than by chance.

Results

Different rates of degradation of ECM gel by PC-3 cells, or PC-3 cells combined with HUVECs, under oxygenated or hypoxic conditions, are evident in the T_1-weighted ^{1}H MR images shown in Figure 2*A*; for the concentration used, DU-145 cells did not demonstrate significant degradation of the ECM gel used in this study (Figure 2*B*). Invasion indices $I(t)$ for MR experiments performed under the different conditions are summarized in Figure 2, *C* and *D*. Continuous hypoxia of up to 3 days resulted in a significant decrease of invasion by PC-3 cells (Figure 2*C*). This decrease of invasion, under hypoxic conditions, was significantly attenuated by the presence of HUVECs, as in the first 1.5 days under hypoxia $I(t)$ of PC-3 cells with HUVECs was significantly higher than $I(t)$ of PC-3 cells alone (Figure 2*C*). Under oxygenated conditions, however, the presence of HUVECs did not alter $I(t)$ of PC-3 cells (Figure 2*C*). In contrast, $I(t)$ of DU-145 cells was not altered significantly by hypoxia or by the presence of HUVECs (Figure 2, *B* and *D*). The results obtained for the enzymatic analysis of MMP-2, MMP-9, and uPA are shown in Figure 3 and in the supplement (Table W1 and Figure W1). The endogenous enzyme activities for MMP-2, MMP-9, and uPA in oxygenated PC-3 cells increased in the presence of HUVECs. Hypoxia increased endogenous MMP-2, MMP-9, and uPA activities in PC-3 cells alone. However, in the presence of HUVECs, the enzyme activities in cells exposed to 48 hours of hypoxia decreased. In both cell types, the contact of the cells to ECM gel was able to alter endogenous MMP-2, MMP-9, and uPA activities (Figure W1). For all experimental conditions, HUVECs demonstrated much higher endogenous MMP-2, MMP-9, and uPA activity per cell than PC-3 cells (Figure W1).

Although the exposure of PC-3 cells to 48 hours of hypoxia resulted in a number of differentially expressed genes related to the invasive and angiogenic phenotype, no change in gene expression levels was observed for MMP-2, MMP-9, and uPA (Figure 4).[4] In addition, several genes associated with cell–cell adhesion, cell–matrix adhesion, migration, and cell motility were downregulated and upregulated in hypoxic PC-3 cells (Figure 4).

In MBC experiments, the changes in cell number, as represented by changes in the intracellular water signal obtained from cellular profiles and ^{1}H MR spectra, indicated that cancer cell proliferation was less under hypoxic than oxygenated conditions (data not shown). Based on the cell count at the start and end of the experiments, we did not observe cell swelling or shrinkage during the MR experiments but the intracellular water signal was proportional to the cell number. Cell cycle analysis revealed a significantly smaller S-phase fraction of hypoxic PC-3 cells than oxygenated PC-3 cells (Figure 5*A*). For HUVECs, which were grown in $RPMI_c$ to maintain consistency with the medium used for cancer cells, exposure to 48 hours of hypoxia lowered the number of cells in the G_0/G_1 phase and increased the number of cells in the G_2/M phase (Figure 5*A*). The small S-phase fraction of oxygenated as well as hypoxic HUVECs may be caused by the use of nonoptimized cell culture medium for the endothelial cells (Figure 5*A*). The use of this medium may have also biased the interaction of HUVECs with the PC-3 cells. Gene expression analysis of PC-3 cells revealed a hypoxia-mediated downregulation of genes involved in the formation of the prereplicative complex during the late M and early G_1 phases of the cell cycle (Figure 5*B*).

Representative 1D ^{31}P MR spectra of PC-3 cells during continuous hypoxia illustrate the stability of pH and energy levels during the MR experiments (Figure 6*A*). The pH remained constant at 7.30 ± 0.15 in all MR experiments. Analysis of β-nucleoside triphosphate levels demonstrated that energy levels remained stable during the course of the MR experiments (data not shown). Interestingly, PCr increased continuously during hypoxia (Figure 6*B*). During the MR experiment, the phospholipid metabolite GPC declined to undetectable levels after an initial increase. This decline was faster for oxygenated PC-3 cells than hypoxic PC-3 cells. These changes in GPC levels were inversely related to $I(t)$ (Figure 6*C*). Additionally, hypoxia led to the upregulation of several genes encoding for proteins essential in glycolysis (Figure 6*D*). Different isoforms of the solute carrier family 2 (facilitated glucose transporter) were either upregulated or downregulated during hypoxia (Figure 6*D*). With hypoxia, several genes that encode for key enzymes of phosphatidylcholine metabolism were downregulated and genes encoding for annexin A1, annexin A3, and peroxiredoxin 6 were upregulated (Figure 6*D*).

Representative localized 1D ^{1}H MR spectra along the sample under the four different experimental conditions and corresponding T_1-weighted ^{1}H MR images are shown in Figure 7. The ECM gel is apparent as a well-defined hyperintense layer in these ^{1}H MR images. The spatial distribution of cellular metabolites, such as tCho, tCr, and LacTG, through the entire sample, including the invading front, was determined from the localized spectra. The spatial distributions of cellular LacTG levels through the sample at days 1, 2, and 3 for oxygenated PC-3 cells, hypoxic PC-3 cells, oxygenated PC-3 cells with HUVECs, and hypoxic PC-3 cells with HUVECs are summarized in Figure 8.

[4] For a complete listing of differentially expressed genes in hypoxic PC-3 cells compared to oxygenated PC-3 cells, see Table W2 (supplemental data available on neoplasia.com).

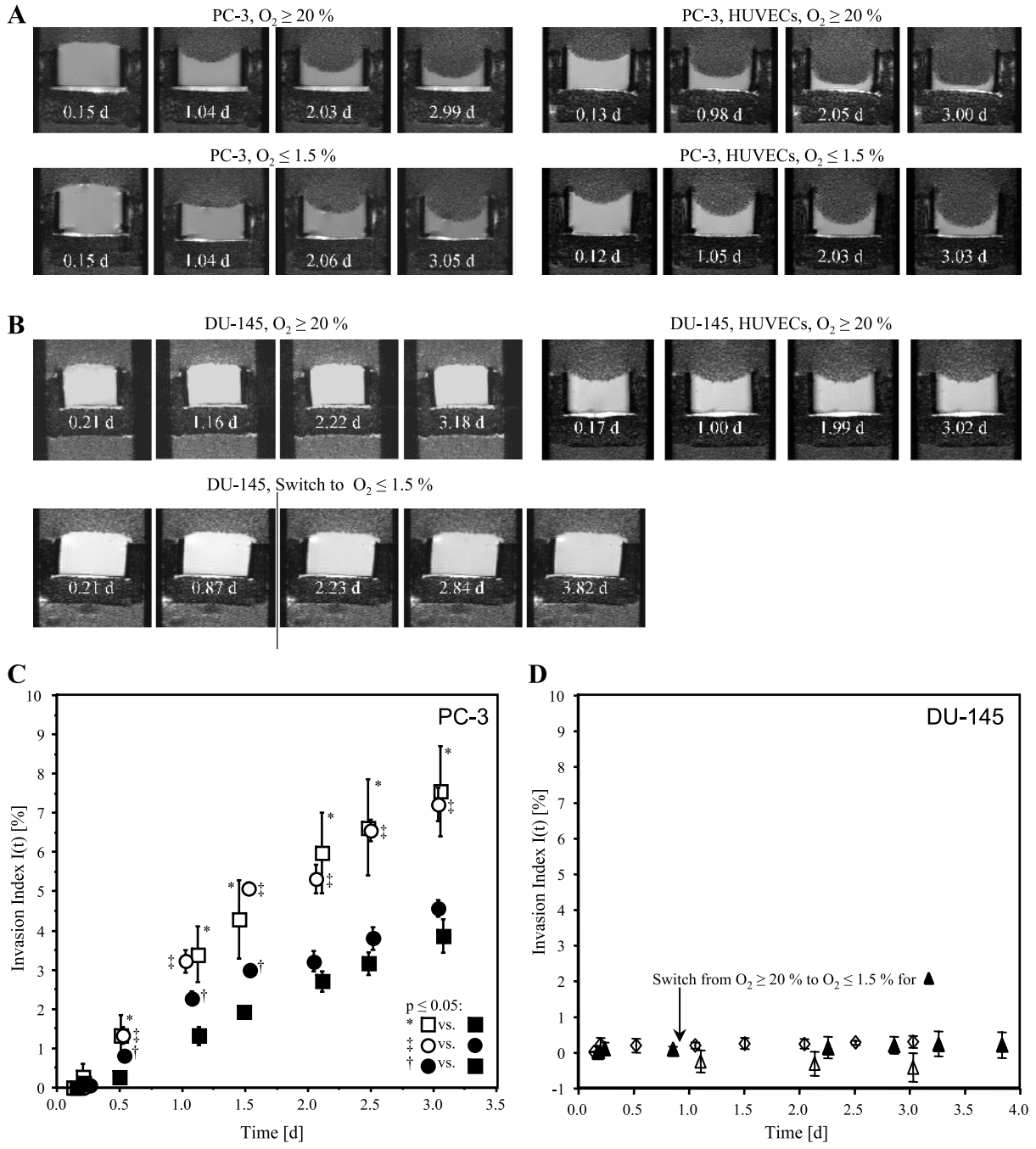

Figure 2. *(A, B) Representative ^{1}H MR images of PC-3 cells alone, PC-3 cells combined with HUVECs, under oxygenated or hypoxic conditions, hypoxic and oxygenated DU-145 cells, and oxygenated DU-145 cells in the presence of HUVECs. The ^{1}H MR images demonstrate differences in degradation of ECM gel by PC-3 under the different conditions (A) but show no visible degradation of the ECM gel by DU-145 cells (B). In experiments with HUVECs, 20 μl less volume of ECM was loaded in the chamber to accommodate the suspension of HUVECs on the surface of the polymerized ECM gel resulting in a concave surface of the ECM gel at the start of the experiments. The resulting differences in the thickness of the ECM gel at the start of the experiments were accounted for in the calculation of the invasion index* I(t). *(C) Invasion index* I(t) versus *time for (□) oxygenated PC-3 cells (n = 4); (○) PC-3 cells in the presence of HUVECs under oxygenated conditions (n = 4); (■) PC-3 cells alone under hypoxia (n = 4); (●) PC-3 cells in the presence of HUVECs under hypoxia (n = 4). (D) Invasion index* I(t) *over time for (△) oxygenated DU-145 (n = 4), (▲) DU-145 exposed to continuous hypoxia starting day 1 (n = 2), and (◇) oxygenated DU-145 in the presence of HUVECs (n = 3). (C, D) Values represent mean ± SEM. The Mann-Whitney U test was performed to test for statistically significant differences (P < .05).*

The data in Figure 8*A* revealed a significant increase of intracellular LacTG at the invading front of oxygenated PC-3 cells in the ECM gel region compared to PC-3 cells outside that region for the first 2 days ($P \leq .0679$, Mann-Whitney U test), but not for day 3. This increase of LacTG levels at the invading front became significantly more pronounced for hypoxic PC-3 cells, and LacTG levels of hypoxic PC-3 cells at the invading front were also significantly ($P = .0679$, Mann-Whitney U test) higher compared to PC-3 cells outside the ECM gel region for days 1 and 2, but not for day 3 (Figure 8*B*). The presence of HUVECs significantly attenuated these increased LacTG levels at the invading front under oxygenated and hypoxic conditions; intracellular LacTG levels were for the most part significantly lower for PC-3 cells

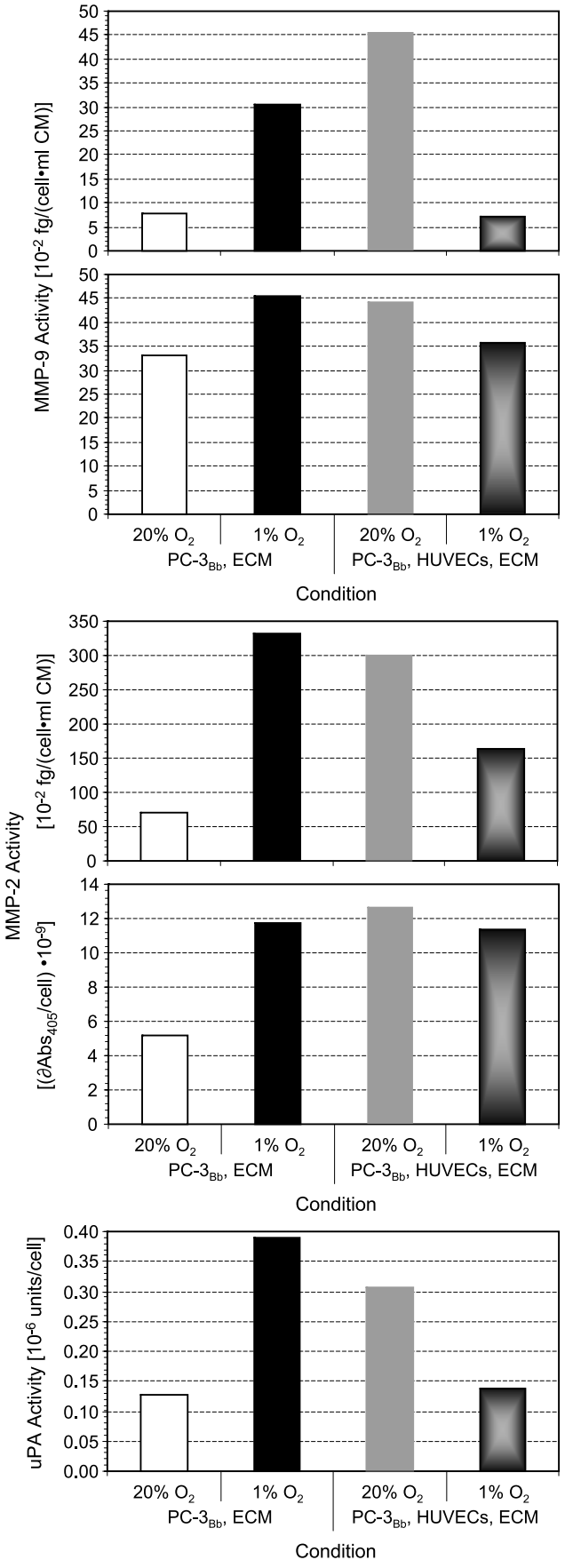

at the invading front compared to PC-3 cells further from it (Figure 8, *C* and *D*).

Levels of intracellular LacTG obtained from global 1D ^{1}H MR spectra are shown in Figure 9*A*. Global intracellular LacTG increased significantly as a result of hypoxia for PC-3 cells alone, as well as for PC-3 cells combined with HUVECs. These data are consistent with the CSI MR data in which, overall, significantly ($P < .05$, Mann-Whitney U test) higher levels of intracellular LacTG were detected under hypoxic conditions for PC-3 cells alone, as well as for PC-3 cells combined with HUVECs. Intracellular Lac increased only slightly under hypoxia, whereas TG levels rose approximately twofold (Figure 9, *B* and *C*). Global, intracellular Lac and TG levels were not significantly altered by the presence of HUVECs (Figure 9, *B* and *C*). As can be seen in Figure 9*D*, exposure of PC-3 cells to 48 hours of hypoxia downregulated a multitude of genes and upregulated only three genes encoding for proteins that are essential for triacylglycerol biosynthesis and use.

Additionally, *HIF1A*, a gene encoding for hypoxia-inducible factor-1 alpha (HIF-1α) subunit, as well as *PH-4* and *HIF1AN*, two genes encoding for hydroxylases involved in the regulation of HIF-1α, were downregulated by hypoxia (see Table W2).

Discussion

Whereas the invasion of minimally invasive DU-145 cells was not significantly influenced by hypoxia in the presence or absence of HUVECs, the four major observations made for PC-3 cells state that 1) hypoxia reduced cancer cell invasion, 2) the presence of HUVECs in the proximity of the cancer cells attenuated this reduction and conferred an advantage in invasion under hypoxia, 3) distinct metabolic changes were detected that were closely related to invasion, and 4) the presence of HUVECs altered the metabolism of cancer cells at the invading front.

We also observed changes in the endogenous enzyme activities of MMP-2, MMP-9, and uPA induced by hypoxia and in coculture experiments combining PC-3 cells and HUVECs. Hypoxia reduced cell proliferation of PC-3 cells.

Microarray analysis of PC-3 cells revealed differential expression of genes related to invasion, angiogenesis, cell adhesion, cell cycle, energy, and lipid metabolism as the result of a hypoxic cell environment. The expression level of a variety of these differentially expressed genes is transcriptionally regulated by HIF-1α [20]. Hypoxia-induced upregulation of genes, such as *VEGF*, *Aldolase A*, *Aldolase C*, or *Enolase 1*, indicated an increase of stabilized HIF-1α [20].

Figure 3. *Endogenous enzyme activities of MMP-9, MMP-2, and uPA for oxygenated and hypoxic PC-3 cells grown adherently on Biosilon beads (PC-3$_{Bb}$) in the absence and presence of HUVECs on the surface of the ECM gel. Whenever the concentration standard resulted in a usable standard curve, concentrations were calculated otherwise the results were reported as absorbance at 405 nm per cell (δAbs$_{405}$/cell) which is proportional to the enzyme activity per cell. A summary and additional data for the different conditions can be found in Table W1 and Figure W1. Each panel represents an independent experiment.*

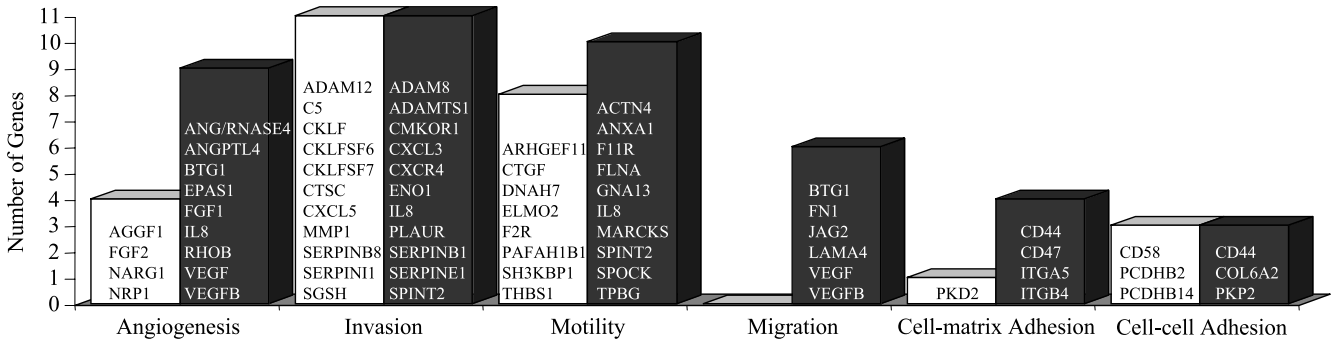

Figure 4. *Genes related to adhesion, motility, migration, invasion, and angiogenesis that have been downregulated (open bar) and upregulated (closed bar) as a result of 48-hour hypoxic (1.0 ± 0.2% O_2) exposure of PC-3 cells in tissue culture compared to oxygenated control cells (20% O_2) (n = 2).*

This does not appear to agree with the lowered gene expression of *HIF1A* in hypoxic cells indicating a reduced production of HIF-1α. However, at the same time, the lowered gene expression of *PH-4* and *HIF1AN* in hypoxic cells indicates reduced expression of hypoxia-inducible factor prolyl 4-hydroxylase and hypoxia-inducible factor 1, alpha subunit inhibitor, two proteins playing a key role in the regulation of HIF-1α expression [20]. The availability of HIF-1α in cells is a combination of HIF-1α synthesis, stabilization, and degradation [20].

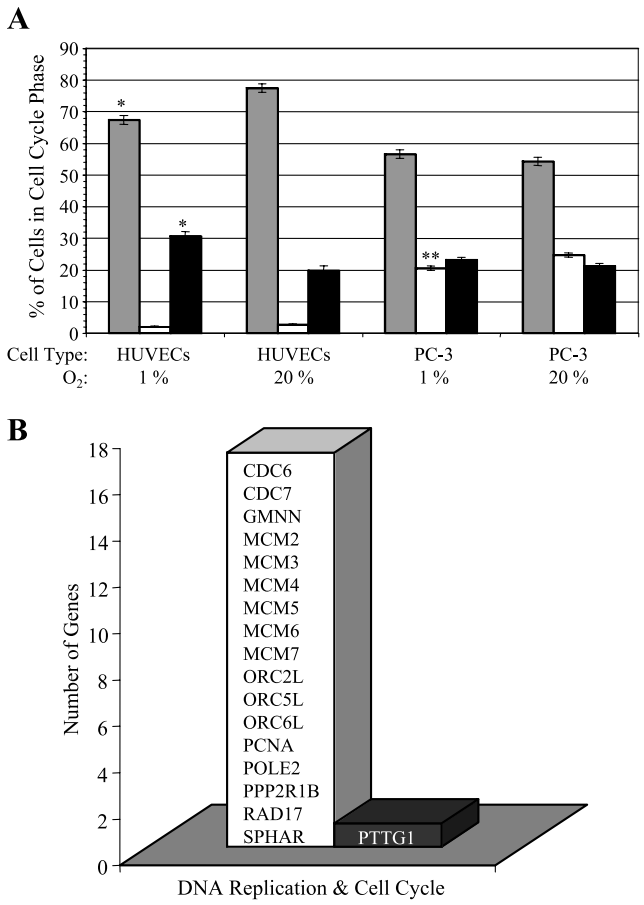

Figure 5. *(A) Percentage of cells in G_0/G_1 phase (gray bar), in S phase (white bar), and in G_2/M phase (black bar) under oxygenated compared to hypoxic conditions (*P ≤ .1, **P ≤ .05). Values represent adjusted means ± SEM from three independent experiments. (B) Genes related to DNA replication in the cell cycle that have been downregulated (open bar) and upregulated (closed bar) as a result of 48-hour hypoxic (1.0 ± 0.2% O_2) exposure of PC-3 cells in tissue culture compared to oxygenated control cells (20% O_2) (n = 2).*

Hypoxia and Invasion

Contrary to observations made in some studies, but consistent with results in other studies, hypoxia significantly decreased the invasion of PC-3 cells. Although such studies have not been performed using PC-3 cells or DU-145 cells, to date, increased invasion with hypoxia has been previously reported in a variety of cancer cells. Graham et al. [21] observed an eightfold increase in invasion of MDA-MB-231 cells during exposure to 24 hours of hypoxia (1% O_2) which coincided with an increase in uPA receptor levels, as determined by flow cytometry. Krishnamachary et al. [22] reported increased invasion into ECM gel by HCT116 human colon carcinoma cells either exposed to hypoxia or overexpressing HIF-1α. He et al. [23] reported that hypoxic exposure of antisense heparanase–transfected clones of a human ovarian carcinoma cell line increased cell invasion. Pennacchietti et al. [24] did not observe any changes in invasion of SiHa (human cervical carcinoma) or U2-OS (human osteosarcoma) cells as a result of 24 hours of hypoxia (3% O_2), but hypoxia in the presence of hepatocyte growth factor stimulated invasion. Sato et al. [25] observed significantly reduced invasion in a human choriocarcinoma cell line following 48 hours of culture under hypoxic conditions. Similarly, Kilburn et al. [26] have observed a threefold decrease in invasion by HTR-8/SV*neo* cells during a 72-hour exposure of these cells to 2% O_2, while Graham et al. [27] detected increased invasion by HTR-8/SV*neo* cells during a 24-hour exposure to 1% O_2. Krtolica and Ludlow [28] observed that 24 hours of hypoxic exposure did not alter the invasion of three ovarian carcinoma cell lines exhibiting different degrees of invasiveness. From these results, it is apparent that the effect of continuous hypoxia on cancer cell invasion is not consistent and can vary from one cell line, or even one study, to another.

Our studies were performed using our novel MR-compatible invasion assay whereas, traditionally, cancer cell invasion has been assessed using the conventional Boyden Chamber assay or modifications thereof [29]. Our MR-compatible assay

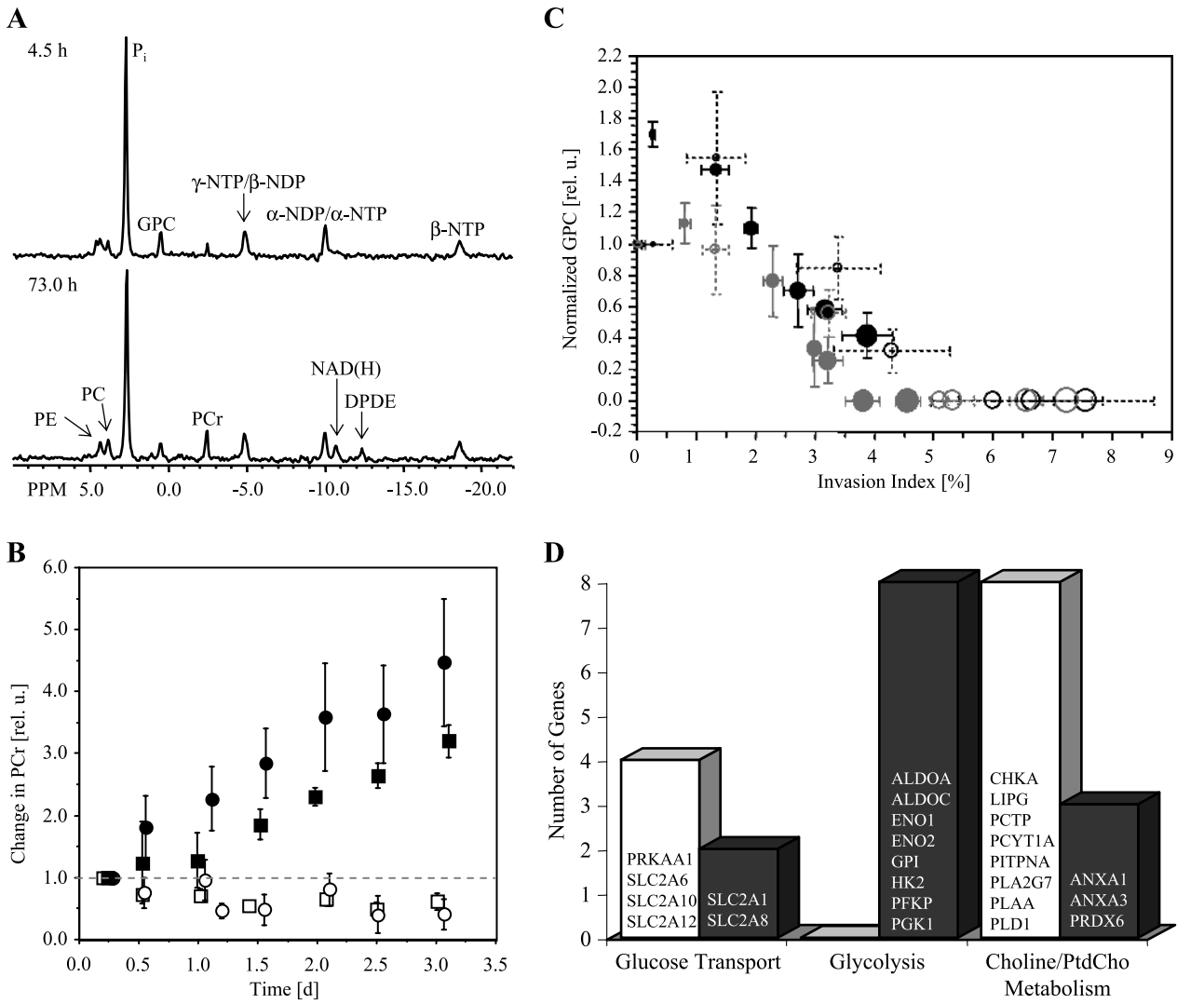

Figure 6. *(A) Representative ^{31}P MR spectra obtained from PC-3 cells maintained under hypoxia. These spectra were obtained at 4.5 and 73 hours of hypoxia, and demonstrated the stability of energy metabolism and pH. Metabolites assigned are:* PE, *phosphoethanolamine;* PC, *phosphocholine;* P_i, *inorganic phosphate;* GPC, *glycerophosphocholine;* PCr, *phosphocreatine;* NTP/NDP, *nucleoside triphosphate/nucleoside diphosphate;* NAD(H), *composed of NAD$^+$, NADH, NADP$^+$, and NADPH;* DPDE, *diphosphodiester. (B) Relative changes of PCr over time for (□) PC-3 cells alone under oxygenated conditions (n = 4); (○) PC-3 cells in the presence of HUVECs under oxygenated conditions (n = 4); (■) PC-3 cells alone under hypoxia (n = 4); (●) PC-3 cells in the presence of HUVECs under hypoxia (n = 4). Values represent mean ± SEM. (C) Correlation between the changes in GPC levels and the invasion index I(t) for (○) oxygenated PC-3 cells, (●) hypoxic PC-3 cells, (○) PC-3 cells combined with HUVECs under oxygenated conditions, and (●) PC-3 cells combined with HUVECs under hypoxia. The diameter of the open or closed circles is directly proportional to the time. Values represent mean ± SEM obtained of four independent experiments. (D) Genes related to glucose transport, the glycolytic pathway, and phosphatidylcholine metabolism that have been downregulated (open bar) and upregulated (closed bar) as a of 48-hour hypoxic (1.0 ± 0.2% O_2) exposure of PC-3 cells in tissue culture compared to oxygenated PC-3 cells (20% O_2) (n = 2).*

was carefully characterized and the measured invasive ability of three human breast and three prostate cancer cell lines agreed with studies performed using the conventional assay [12,13]. Therefore, it is unlikely that the decreased invasion detected in hypoxic PC-3 cells is an artifact.

We observed that not only hypoxia but also the presence of ECM gel or the coculture of PC-3 cells and HUVECs altered the endogenous enzyme activities of MMP-2, MMP-9, and uPA. These changes in enzyme activities did not support the notion that increased endogenous activity of selected ECM-degrading proteases automatically results in increased cancer cell invasion. These findings are consistent with *in vivo* and *in vitro* experiments demonstrating that the presence of stromal components, such as ECM, endothelial cells, fibroblasts, can significantly affect cancer invasion, metastasis, and enzyme activities in cancer cells or tumors [1,7]. Furthermore, recent research has demonstrated that the proteolytic activity of ECM-degrading proteases is not restricted to just ECM proteins as targets but can generate bioactive protein fragments, or stimulate cell–cell dissociation, or cell apoptosis, or endothelial cell proliferation [3,7].

In our microarray experiments, we found a number of genes related to adhesion, invasion, and angiogenesis, to be upregulated and downregulated under hypoxia. Most notably, we did not find significant changes in *uPAR*, *MMP9*, and *MMP2* gene expression levels, despite compelling evidence suggesting a modulating role for these genes in cancer cell invasion [4,30]. However, other genes encoding for MMPs,

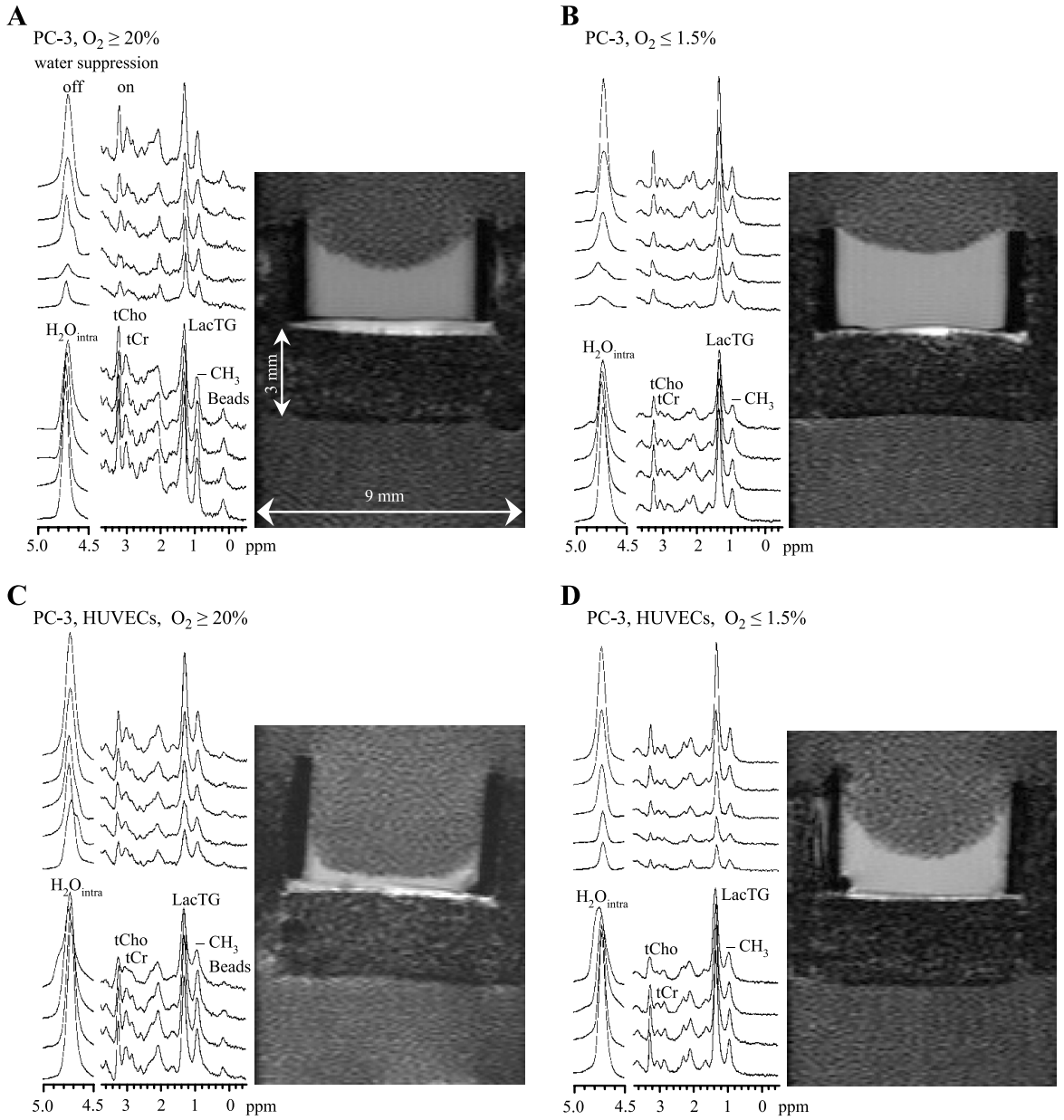

Figure 7. *Representative 1D ^{1}H CSI spectra of 310-μm-thick slices (every third spectrum is shown) obtained along the sample at 47 hours, acquired with or without water suppression, together with the corresponding ^{1}H MR images for (A) oxygenated PC-3 cells, (B) hypoxic PC-3 cells, (C) PC-3 cells in the presence of HUVECs under oxygenated conditions, and (D) PC-3 cells in the presence of HUVECs under hypoxia.*

such as *MMP1* and *MMP16*, were downregulated and this downregulation may have contributed to the observed changes in invasion [31,32]. Together, the results of the enzyme activity assay and gene microarray experiments indicate 1) that the expression of active proteolytic enzymes may be regulated posttranslationally and 2) that the interplay between multiple proteases expressed by cancer and stromal cells as well as differences between 2D and 3D environments may regulate the ability of cancer cells to invade ECM [33].

Compared to oxygenated conditions, hypoxia reduced cell proliferation of PC-3 cells in our MR experiments. This observation was supported by the lower number of cells on beads counted at the end of the perfusion study, by the cell cycle analysis, and by the hypoxia-induced downregulation of *Geminin*, *MCM2–7*, and *ORC* genes observed by microarray analysis. *Geminin*, *MCM*, and *ORC* genes encode for proteins that are essential for DNA replication in the cell cycle [34].

Our observations agree with previous reports that hypoxia downregulates DNA synthesis [10] and that hypoxia is able to reversibly suppress replicon initiation as well as reversibly slow down the progress rates of replication forks in HeLa cells and CCRF-CEM cells [35].

Endothelial Cell/Cancer Cell Interaction and Invasion

The presence of HUVECs in the proximity of oxygenated DU-145 cells or PC-3 cells did not affect their invasion. Our results are consistent with studies by Scott et al. [36] in which PC-3 cell invasion did not change in response to the addition

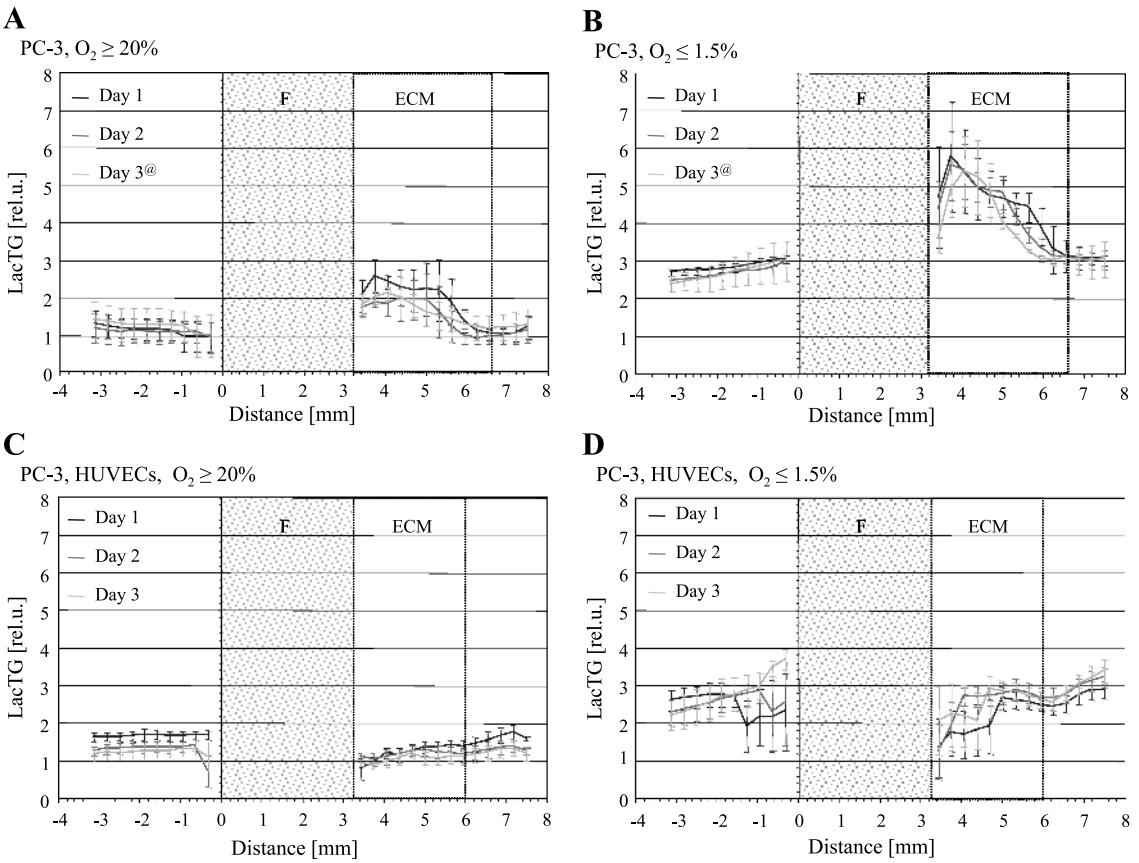

Figure 8. *Relative levels of lactate and triglycerides (LacTG) along the sample obtained for (A) oxygenated PC-3 cells, (B) hypoxic PC-3 cells, (C) PC-3 cells in the presence of HUVECs under oxygenated conditions, and (D) PC-3 cells in the presence of HUVECs under hypoxia. Values, presented as mean ± SEM, are from localized 1D ^{1}H MR spectra averaged over four experiments for each condition, unless for time points marked with an at sign (@), which were averaged over three independent MR experiments. The base of the ECM gel chamber was defined as 0 mm.* F *represents the thickness of filter material forming the base of the ECM gel chamber;* ECM*, the thickness of ECM gel at the start of the MR experiments.*

of HUVECs, although PC-3 cell invasion did increase in response to bone marrow endothelial cells or bone marrow stromal cells. Because the endothelial cell layer can vary from organ to organ [19], it is possible that substituting HUVECs for microvascular endothelial cells derived from normal or malignant prostatic tissue may result in increased invasion, even under oxygenated conditions.

Whereas the presence of endothelial cells in the proximity of minimally invasive DU-145 cells did not affect their invasion under hypoxia, HUVECs did, however, confer an advantage in invasion of hypoxic PC-3 cells. This advantage was primarily related to endothelial cell/cancer cell interaction, because HUVECs alone did not increase degradation of ECM gel under hypoxia. Whereas the presence of cyclic or chronic hypoxia in the vicinity of endothelial cells may not be anticipated in healthy tissue, in tumors, endothelial cells are frequently observed in regions adjacent to necrosis (e.g., [4]). Also, chronic or cyclic hypoxia can occur in tumors due to intermittent vascular collapse or following radiation therapy during reoxygenation [4].

In control experiments, oxygenated or hypoxic HUVECs alone did not degrade ECM gel. These results are consistent with a study performed using a different MR-based invasion system demonstrating that oxygenated HUVECs invaded ECM gel only in the presence of cancer cells [16].

Metabolism and Invasion

In normal hypoxic cells, intracellular ATP levels typically decrease as mitochondrial oxidative phosphorylation becomes limited, and the high-energy phosphate metabolite, PCr, the energy reservoir of the cell, is rapidly consumed in an effort to keep up with the energy demand of the cell [37]. As energy becomes limited, two major ATP-consuming processes, i.e., protein synthesis and RNA/DNA synthesis, fall off sharply, whereas ion-regulating ATPases, such as Na^+/K^+-ATPase or Ca^{2+}-ATPase, take priority [38]. In parallel with decreased invasion, nucleoside triphosphate levels in our study remained constant and PCr increased in PC-3 cells during hypoxia. Also, oxygen levels along the sample remained virtually unchanged for PC-3 cells (data not shown), indicating that PC-3 cells have a low oxygen consumption rate and most likely derive ATP mainly through glycolysis, even under oxygenated conditions (Warburg effect [39]). The trend toward increased intracellular Lac in PC-3 cells under hypoxia may be due to increased glycolytic activity as a result of hypoxia. This is further supported by the upregulation of genes encoding for proteins in the glycolytic pathway in response to hypoxia, as observed in the microarray analysis. Most of these genes contain an HIF-1 binding site, and thus, HIF-1 is most likely the major factor responsible for the hypoxia-sensitive regulation of glycolytic enzyme genes [40]. The changes in

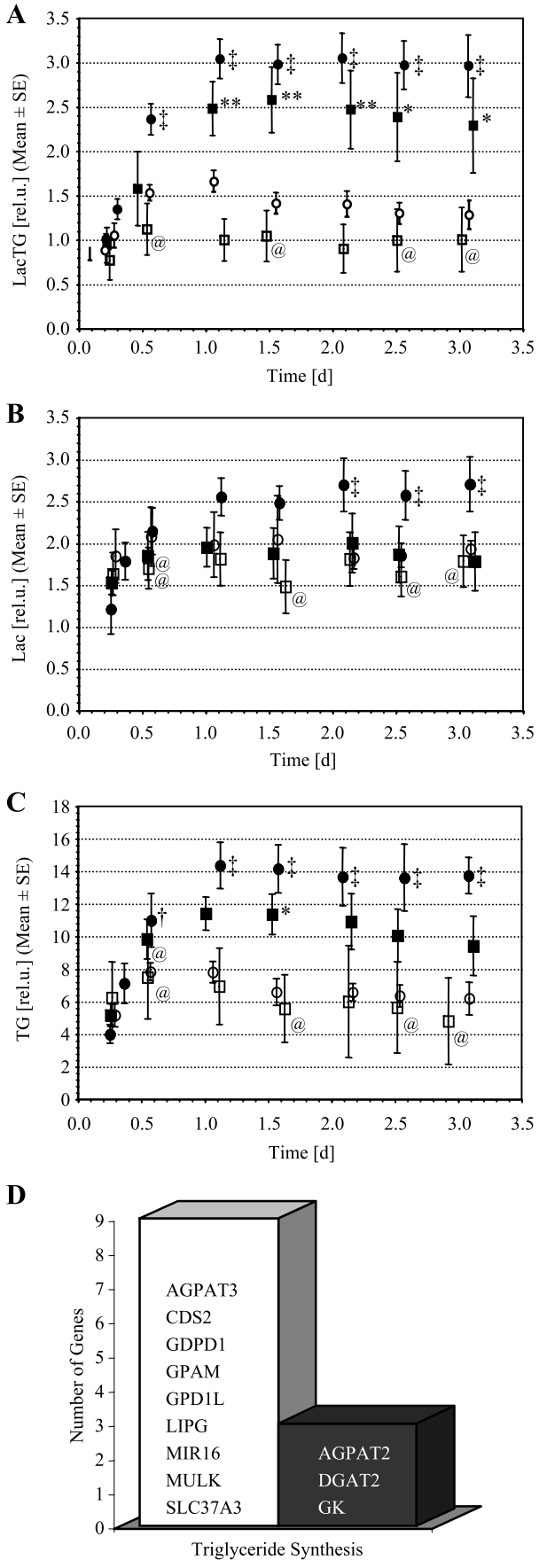

glucose transporter gene expression levels observed as a result of hypoxia suggest altered glucose transport. Increased expression of GLUT1 (SLC2A1) has been shown to relate to cancer progression and hypoxia [41]. Currently, only limited information is available on the class II GLUT isoforms (SLCA2A6, SLCA2A8, SLCA2A10, and SLCA2A12) [42].

Reduced ATP consumption combined with low oxygen demand and a high rate of glycolytic activity appeared to be sufficient to meet the energy requirements of hypoxic PC-3 cells. Continued synthesis of PCr and decreased PCr consumption may have led to the accumulation of PCr under hypoxia. Therefore, in PC-3 cells, the reduced invasion and proliferation observed under hypoxia was not due to de-energization of the cancer cells, but may be explained by the downregulation of ATP-consuming processes.

The inverse relationship between changes in GPC levels and the invasion index was consistent with previous findings that treatment of cancer cells with the anti-inflammatory agent indomethacin reduced invasion ([14,43], and references therein) and increased GPC ([14], and references therein). Under hypoxia, the downregulation of genes encoding for proteins of the cytidine diphosphocholine metabolism, phosphatidyltransfer protein, and phospholipases indicated a reduction of phosphatidylcholine turnover [44,45]. Additionally, hypoxia-upregulated gene expression of annexin A1 and A3 can be followed by inhibition of phospholipase activity [46]. Both processes could influence the changes in GPC. However, the functional context of genes related to phosphatidylcholine metabolism and their expression levels, especially under hypoxia, is largely unexplored and warrants further investigations [47].

Endothelial Cell–Cancer Cell Interaction and Metabolism

The increase of intracellular LacTG in PC-3 cells at the invading front disappeared when HUVECs were present on the ECM gel. This suggests that the endothelial cells triggered the cancer cells to use TG as a substrate, to reduce lactate production, or to export lactate more efficiently. It is unlikely that the metabolic signals from HUVECs caused the differences in the localized MR spectra. The concentration of HUVECs on the ECM gel (5×10^4 cells) is below MR-detectable limits. We have previously observed that cancer cells secrete factors that alter the metabolism of HUVECs [48]. Here, we observed that HUVECs altered the metabolism of cancer cells. The molecular processes underlying the

Figure 9. *Intracellular (A) LacTG, (B) Lac, and (C) TG, calculated from global 1D ^{1}H MR spectra. Note that the relative scale in (A) acquired with a stimulated echo acquisition mode–based pulse sequence differs from (B) and (C), which were acquired with a lactate-edited SE-based pulse sequence. (□) PC-3 cells alone under oxygenated conditions (n = 4); (○) PC-3 cells in the presence of HUVECs under oxygenated conditions (n = 4); (■) PC-3 cells alone under hypoxia (n = 4); (●) PC-3 cells in the presence of HUVECs under hypoxia (n = 4). Values represent mean ± SEM. At sign (@), time points at which values of only three independent experiments were available. **P < .05, *P < .1, □ versus ■; ‡P < .05, †P < .1, ○ versus ● (Mann-Whitney U Test). (D) Genes related to triglyceride synthesis that have been downregulated (open bar) and upregulated (closed bar) as a result of 48-hour hypoxic (1.0 ± 0.2% O_2) exposure of PC-3 cells in tissue culture compared to oxygenated control cells (20% O_2) (n = 2).*

downregulation of LacTG at the invading front of cancer cells by the presence of endothelial cells remain to be understood. These data demonstrate the ability of CSI to reveal metabolic differences at the invading front, which were masked in the global spectra of the cells, where a significant increase in intracellular LacTG was detected under hypoxia for both PC-3 alone, as well as for PC-3 cells combined with HUVECs. This increase in LacTG was most likely due to an increase in lactate as well as TG. In eukaryotes, TG acts as an energy source as well as a repository of fatty acids and phospholipid precursors [49]. Furthermore, TG synthesis is believed to protect cells from the potential toxicity of sudden increase of intracellular fatty acids and acyl-CoAs [49]. An ischemic insult in the heart has been shown to increase neutral lipids, with β oxidation as the rate-limiting step for fatty acid oxidation [50]. The exposure of a human fibrosarcoma cell line to 1% O_2 increased the number and size of lipid droplets per cell, the relative amounts of newly synthesized TG, and the intracellular amount of TG compared to oxygenated cells [51]. Because TG can act as an energy source and cell protectant, the limitation of available oxygen may have decreased their use and increased their synthesis.

In summary, these data demonstrate that hypoxia can reduce the invasion of cancer cells, but the presence of endothelial cells can ameliorate this reduction in invasion. Thus, the presence of HUVECs can significantly influence the outcome of cancer cell invasion. Also, our results suggest that, at least for some tumors, therapies that result in reoxygenation or increased oxygenation within the tumor may promote invasion of the ECM, whereas therapies, which reduce oxygenation, may suppress invasion. The endogenous activity of selected extracellular proteases, although influenced by hypoxia, did not fully explain the observed hypoxia-induced changes in invasion. The importance of metabolic pathways, such as the accumulation and use of TG and changes in GPC in the invasive process, require further investigation. Gene expression profiling indicated that multiple cellular functions and pathways are influenced by hypoxia.

Collectively, these data demonstrate the complexity of the hypoxia response and the importance of functional imaging assays to evaluate phenotypic endpoints of cancer cells such as invasion and the ability to degrade ECM, in response to microenvironmental stimuli, such as hypoxia.

Acknowledgements

We thank D.C. Shungu and X. Mao from the Hatch NMR Research Center for providing us with the XsOsNMR software; V.P. Chacko, J. Gillen, and C.C. Talbot, Jr., for their expert technical assistance; and K. Glunde and M. McAllister for critically reading the manuscript.

References

[1] Bissell MJ and Radisky D (2001). Putting tumours in context. *Nat Rev Cancer* **1**, 46–54.

[2] Liotta LA and Kohn EC (2001). The microenvironment of the tumour–host interface. *Nature* **411**, 375–379.

[3] Cairns RA, Khokha R, and Hill RP (2003). Molecular mechanisms of tumor invasion and metastasis: an integrated view. *Curr Mol Med* **3**, 659–671.

[4] Subarsky P and Hill RP (2003). The hypoxic tumour microenvironment and metastatic progression. *Clin Exp Metastasis* **20**, 237–250.

[5] Friedl P and Brocker EB (2000). The biology of cell locomotion within three-dimensional extracellular matrix. *Cell Mol Life Sci* **57**, 41–64.

[6] Pouyssegur J, Dayan F, and Mazure NM (2006). Hypoxia signalling in cancer and approaches to enforce tumour regression. *Nature* **441**, 437–443.

[7] DeClerck YA, Mercurio AM, Stack MS, Chapman HA, Zutter MM, Muschel RJ, Raz A, Matrisian LM, Sloane BF, Noel A, et al. (2004). Proteases, extracellular matrix, and cancer: a workshop of the path B study section. *Am J Pathol* **164**, 1131–1139.

[8] Skrzydlewska E, Sulkowska M, Koda M, and Sulkowski S (2005). Proteolytic–antiproteolytic balance and its regulation in carcinogenesis. *World J Gastroenterol* **11**, 1251–1266.

[9] Festuccia C, Dolo V, Guerra F, Violini S, Muzi P, Pavan A, and Bologna M (1998). Plasminogen activator system modulates invasive capacity and proliferation in prostatic tumor cells. *Clin Exp Metastasis* **16**, 513–528.

[10] Papandreou I, Powell A, Lim AL, and Denko N (2005). Cellular reaction to hypoxia: sensing and responding to an adverse environment. *Mutat Res* **569**, 87–100.

[11] Gehlsen KR, Wagner HN Jr, and Hendrix MJ (1984). Membrane invasion culture system (MICS). *Med Instrum* **18**, 268–271.

[12] Bhujwalla ZM, Artemov D, Natarajan K, Ackerstaff E, and Solaiyappan M (2001). Vascular differences detected by MRI for metastatic *versus* nonmetastatic breast and prostate cancer xenografts. *Neoplasia* **3**, 143–153.

[13] Pilatus U, Ackerstaff E, Artemov D, Mori N, Gillies RJ, and Bhujwalla ZM (2000). Imaging prostate cancer invasion with multi-nuclear magnetic resonance methods: the Metabolic Boyden Chamber. *Neoplasia* **2**, 273–279.

[14] Ackerstaff E, Gimi B, Artemov D, and Bhujwalla ZM (2007). Anti-inflammatory agent indomethacin reduces invasion and alters metabolism in a human breast cancer cell line. *Neoplasia* **9**, 222–235.

[15] Webber MM, Bello D, and Quader S (1997). Immortalized and tumorigenic adult human prostatic epithelial cell lines: characteristics and applications, Part 2. Tumorigenic cell lines. *Prostate* **30**, 58–64.

[16] Gimi B, Mori N, Ackerstaff E, Frost EE, Bulte JW, and Bhujwalla ZM (2006). Noninvasive MRI of endothelial cell response to human breast cancer cells. *Neoplasia* **8**, 207–213.

[17] Kuzuya M, Satake S, Miura H, Hayashi T, and Iguchi A (1996). Inhibition of endothelial cell differentiation on a glycosylated reconstituted basement membrane complex. *Exp Cell Res* **226**, 336–345.

[18] Pathak AP, Gimi B, Glunde K, Ackerstaff E, Artemov D, and Bhujwalla ZM (2004). Molecular and functional imaging of cancer: advances in MRI and MRS. *Methods Enzymol* **386**, 3–60.

[19] Hewett PW and Murray JC (1993). Human microvessel endothelial cells: isolation, culture and characterization. *In Vitro Cell Dev Biol Anim* **29A**, 823–830.

[20] Semenza GL (2004). Hydroxylation of HIF-1: oxygen sensing at the molecular level. *Physiology (Bethesda)* **19**, 176–182.

[21] Graham CH, Forsdike J, Fitzgerald CJ, and Macdonald-Goodfellow S (1999). Hypoxia-mediated stimulation of carcinoma cell invasiveness via upregulation of urokinase receptor expression. *Int J Cancer* **80**, 617–623.

[22] Krishnamachary B, Berg-Dixon S, Kelly B, Agani F, Feldser D, Ferreira G, Iyer N, LaRusch J, Pak B, Taghavi P, et al. (2003). Regulation of colon carcinoma cell invasion by hypoxia-inducible factor 1. *Cancer Res* **63**, 1138–1143.

[23] He X, Brenchley PE, Jayson GC, Hampson L, Davies J, and Hampson IN (2004). Hypoxia increases heparanase-dependent tumor cell invasion, which can be inhibited by antiheparanase antibodies. *Cancer Res* **64**, 3928–3933.

[24] Pennacchietti S, Michieli P, Galluzzo M, Mazzone M, Giordano S, and Comoglio PM (2003). Hypoxia promotes invasive growth by transcriptional activation of the *met* protooncogene. *Cancer Cell* **3**, 347–361.

[25] Sato Y, Fujiwara H, Higuchi T, Yoshioka S, Tatsumi K, Maeda M, and Fujii S (2002). Involvement of dipeptidyl peptidase IV in extravillous trophoblast invasion and differentiation. *J Clin Endocrinol Metab* **87**, 4287–4296.

[26] Kilburn BA, Wang J, Duniec-Dmuchkowski ZM, Leach RE, Romero R, and Armant DR (2000). Extracellular matrix composition and hypoxia regulate the expression of HLA-G and integrins in a human trophoblast cell line. *Biol Reprod* **62**, 739–747.

[27] Graham CH, Fitzpatrick TE, and McCrae KR (1998). Hypoxia stimulates urokinase receptor expression through a heme protein–dependent pathway. *Blood* **91**, 3300–3307.
[28] Krtolica A and Ludlow JW (1996). Hypoxia arrests ovarian carcinoma cell cycle progression, but invasion is unaffected. *Cancer Res* **56**, 1168–1173.
[29] Boyden S (1962). Chemotactic effect of mixtures of antibody and antigen on polymorphonuclear leucocytes. *J Exp Med* **115**, 453–466.
[30] Sahai E (2005). Mechanisms of cancer cell invasion. *Curr Opin Genet Dev* **15**, 87–96.
[31] Zeng ZZ, Jia Y, Hahn NJ, Markwart SM, Rockwood KF, and Livant DL (2006). Role of focal adhesion kinase and phosphatidylinositol 3′-kinase in integrin fibronectin receptor–mediated, matrix metalloproteinase-1–dependent invasion by metastatic prostate cancer cells. *Cancer Res* **66**, 8091–8099.
[32] Sato H, Okada Y, and Seiki M (1997). Membrane-type matrix metalloproteinases (MT-MMPs) in cell invasion. *Thromb Haemost* **78**, 497–500.
[33] Deryugina EI and Quigley JP (2006). Matrix metalloproteinases and tumor metastasis. *Cancer Metastasis Rev* **25**, 9–34.
[34] Tachibana KE, Gonzalez MA, and Coleman N (2005). Cell-cycle–dependent regulation of DNA replication and its relevance to cancer pathology. *J Pathol* **205**, 123–129.
[35] Probst G, Riedinger HJ, Martin P, Engelcke M, and Probst H (1999). Fast control of DNA replication in response to hypoxia and to inhibited protein synthesis in CCRF-CEM and HeLa cells. *Biol Chem* **380**, 1371–1382.
[36] Scott LJ, Clarke NW, George NJ, Shanks JH, Testa NG, and Lang SH (2001). Interactions of human prostatic epithelial cells with bone marrow endothelium: binding and invasion. *Br J Cancer* **84**, 1417–1423.
[37] Erecinska M and Silver IA (1994). Ions and energy in mammalian brain. *Prog Neurobiol* **43**, 37–71.
[38] Boutilier RG (2001). Mechanisms of cell survival in hypoxia and hypothermia. *J Exp Biol* **204**, 3171–3181.
[39] Warburg O (1956). Respiratory impairment in cancer cells. *Science* **124**, 269–270.
[40] Webster KA (2003). Evolution of the coordinate regulation of glycolytic enzyme genes by hypoxia. *J Exp Biol* **206**, 2911–2922.
[41] Macheda ML, Rogers S, and Best JD (2005). Molecular and cellular regulation of glucose transporter (GLUT) proteins in cancer. *J Cell Physiol* **202**, 654–662.
[42] Uldry M and Thorens B (2004). The SLC2 family of facilitated hexose and polyol transporters. *Pflugers Arch* **447**, 480–489.
[43] Nithipatikom K, Isbell MA, Lindholm PF, Kajdacsy-Balla A, Kaul S, and Campell WB (2002). Requirement of cyclooxygenase-2 expression and prostaglandins for human prostate cancer cell invasion. *Clin Exp Metastasis* **19**, 593–601.
[44] Ackerstaff E, Glunde K, and Bhujwalla ZM (2003). Choline phospholipid metabolism: a target in cancer cells? *J Cell Biochem* **90**, 525–533.
[45] Zeisel SH (1993). Choline phospholipids: signal transduction and carcinogenesis. *FASEB J* **7**, 551–557.
[46] Wallner BP, Mattaliano RJ, Hession C, Cate RL, Tizard R, Sinclair LK, Foeller C, Chow EP, Browing JL, Ramachandran KL, et al. (1986). Cloning and expression of human lipocortin, a phospholipase A_2 inhibitor with potential anti-inflammatory activity. *Nature* **320**, 77–81.
[47] Glunde K, Jie C, and Bhujwalla ZM (2004). Molecular causes of the aberrant choline phospholipid metabolism in breast cancer. *Cancer Res* **64**, 4270–4276.
[48] Mori N, Natarajan K, Chacko VP, Artemov D, and Bhujwalla ZM (2003). Choline phospholipid metabolites of human vascular endothelial cells altered by cyclooxygenase inhibition, growth factor depletion, and paracrine factors secreted by cancer cells. *Mol Imaging* **2**, 124–130.
[49] Coleman RA and Lee DP (2004). Enzymes of triacylglycerol synthesis and their regulation. *Prog Lipid Res* **43**, 134–176.
[50] Whitmer JT, Idell-Wenger JA, Rovetto MJ, and Neely JR (1978). Control of fatty acid metabolism in ischemic and hypoxic hearts. *J Biol Chem* **253**, 4305–4309.
[51] Goto K, Asai T, Hara S, Namatame I, Tomoda H, Ikemoto M, and Oku N (2005). Enhanced antitumor activity of xanthohumol, a diacylglycerol acyltransferase inhibitor, under hypoxia. *Cancer Lett* **219**, 215–222.

Table W1. Changes in Endogenous Enzyme Activities for PC-3 Cells and HUVECs under Different Conditions in Relation to the Invasion Index Measurements.

Experimental Condition	Invasion Index $I(t)$ (MR Experiments)	Endogenous Enzyme Activity per Cell of		
		MMP-2	MMP-9	uPA
$PC\text{-}3_{Bb}$ on ECM	20% O_2 > 1% O_2	20% O_2 < 1% O_2	20% O_2 < 1% O_2	20% O_2 < 1% O_2
$PC\text{-}3_T$	N/A	20% O_2 < 1% O_2	20% O_2 < 1% O_2	20% O_2 < 1% O_2
$PC\text{-}3_{Bb}$ on HuvECM	20% O_2 > 1% O_2	20% O_2 > 1% O_2	20% O_2 > 1% O_2	20% O_2 > 1% O_2
PC-3, 20% O_2	N/A	Plastic > ECM	Plastic > ECM	Plastic > ECM
PC-3, 1% O_2	N/A	Inconclusive	Plastic ≤ ECM	Plastic < ECM
$PC\text{-}3_{Bb}$, 20% O_2	ECM = HuvECM	Inconclusive	ECM < HuvECM	ECM ≤ HuvECM
$PC\text{-}3_{Bb}$, 1% O_2	ECM < HuvECM	ECM ≥ HuvECM	ECM > HuvECM	ECM > HuvECM
HuvECM	N/A	20% O_2 > 1% O_2	20% O_2 = 1% O_2	20% O_2 ≤ 1% O_2
$HUVECs_T$	N/A	20% O_2 > 1% O_2	20% O_2 > 1% O_2	20% O_2 > 1% O_2
HUVECs, 20% O_2	N/A	Plastic < ECM	Inconclusive	Plastic > ECM
HUVECs, 1% O_2	N/A	Plastic < ECM	Plastic < ECM	Plastic ≤ ECM
No. of experiments	$n = 4$	$n = 2$	$n = 2$	$n = 1$

For all experimental conditions, HUVECs expressed much higher endogenous MMP-2, MMP-9, and uPA activity per cell than PC-3 cells (data shown in Figure W1, *A*–*C*).

$PC\text{-}3_{Bb}$, PC-3 cells grown adherently on Biosilon beads; *$PC\text{-}3_T$*, PC-3 cells grown adherently on tissue culture plastic; *HuvECM*, HUVECs on ECM gel; *$HUVECs_T$*, HUVECs grown adherently on tissue culture plastic; *N/A*, not applicable.

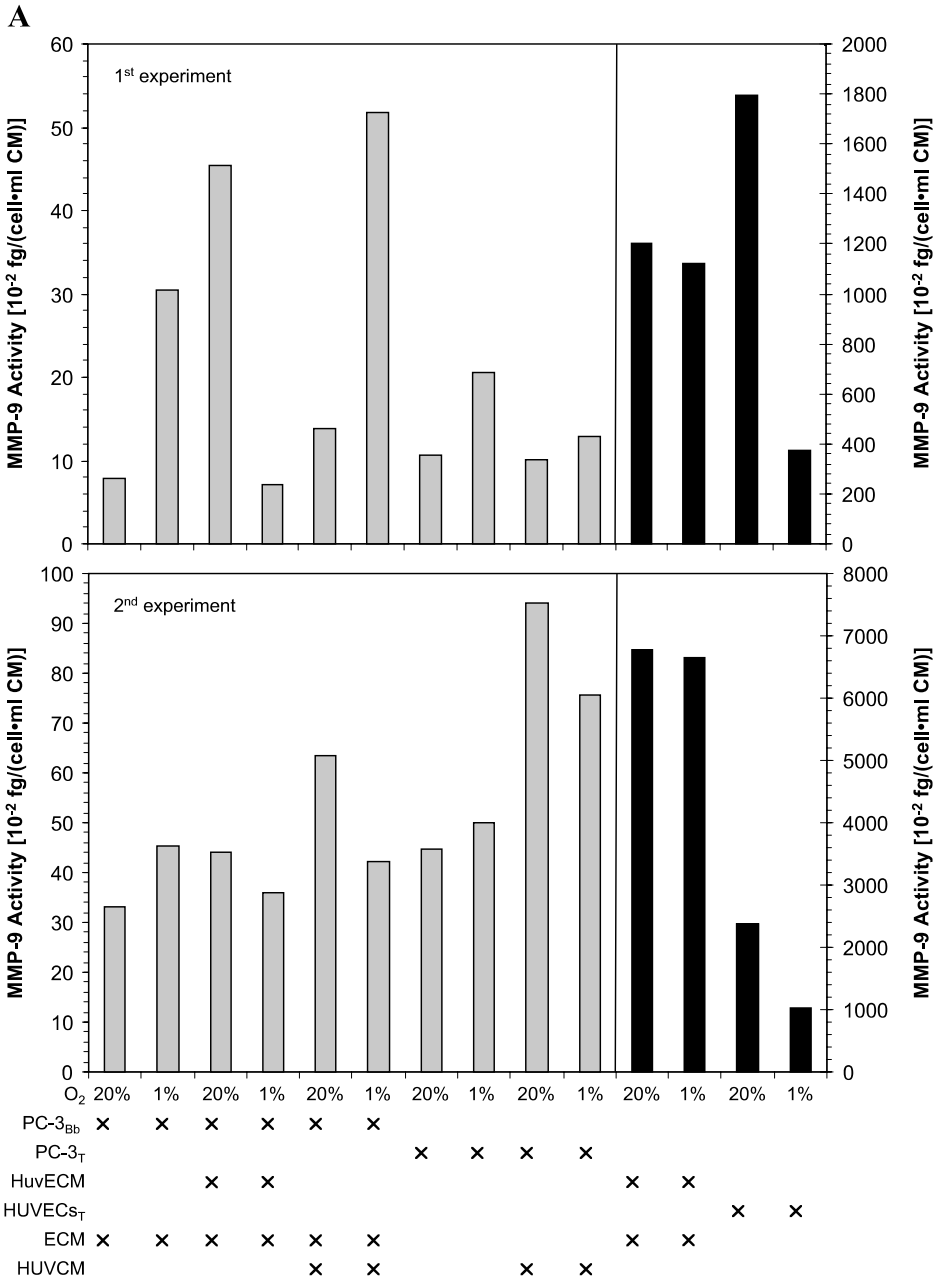

Figure W1. *Endogenous (A) MMP-9, (B) MMP-2, and (C) uPA activities for PC-3 cells and HUVECs under different conditions, from two independent experiments. HUVECs expressed much higher endogenous MMP-9, MMP-2, and uPA activity per cell than PC-3 cells.* PC-3_{Bb}, *PC-3 cells grown adherently on Biosilon beads;* PC-3_T, *PC-3 cells grown adherently on tissue culture plastic;* HuvECM, *HUVECs on ECM gel;* $HUVECs_T$, *HUVECs grown adherently on tissue culture plastic;* HUVCM, *HUVEC-conditioned cell culture medium; black bars corresponding to y-axis to the right, gray bars corresponding to y-axis to the left. The cell culture medium was RPMI 1640 supplemented with 9% FBS, 90 U/ml penicillin, and 90 μg/ml streptomycin. [1]In the second experiment, the MMP-2 standard delivered not a usable standard curve to calculate the concentrations. However, the enzyme activity per cell is directly proportional to the absorbance at 405 nm per cell (δAbs_{405}/ cell) still allowing the comparison of the different conditions if not absolute quantification.*

B

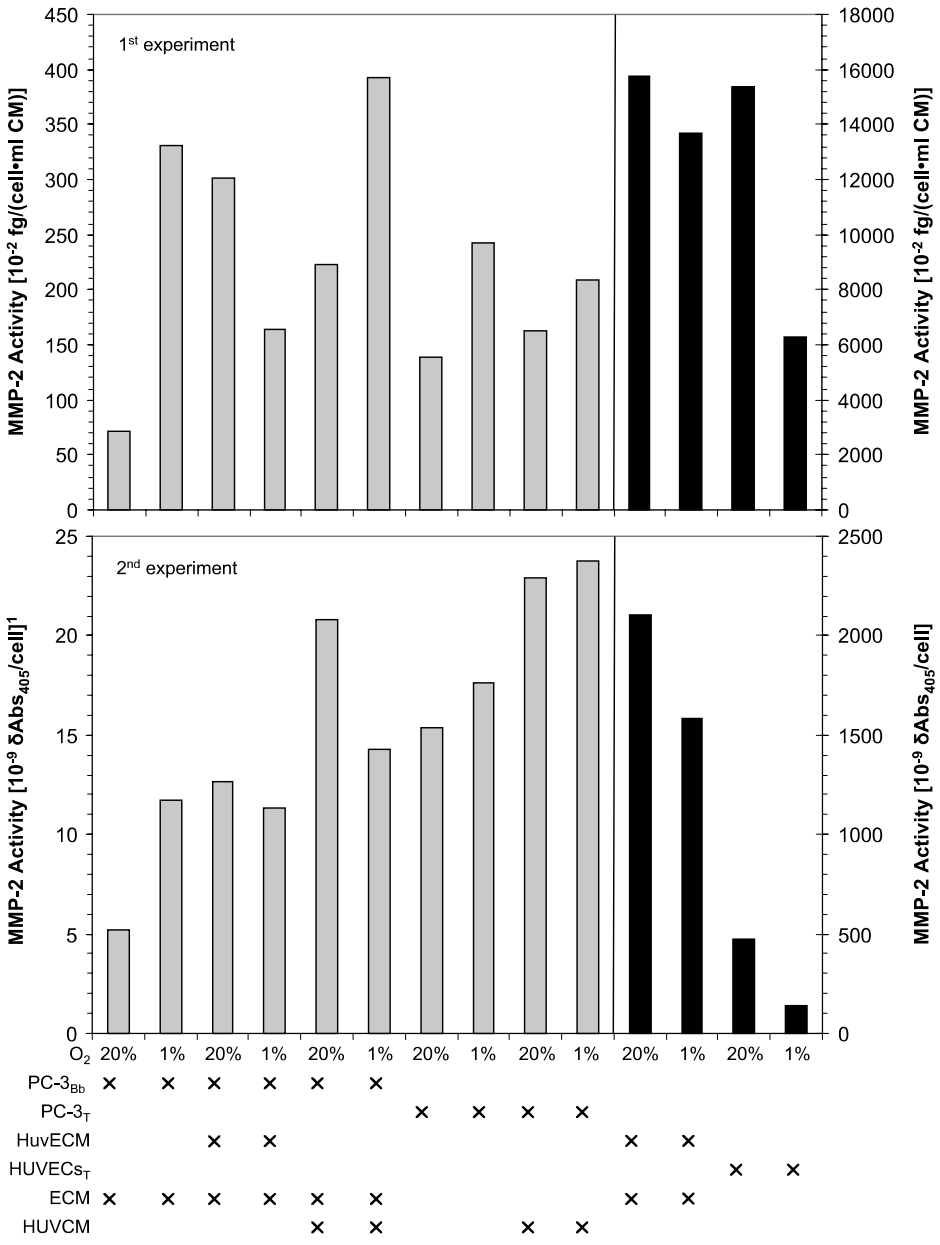

Figure W1. *(continued).*

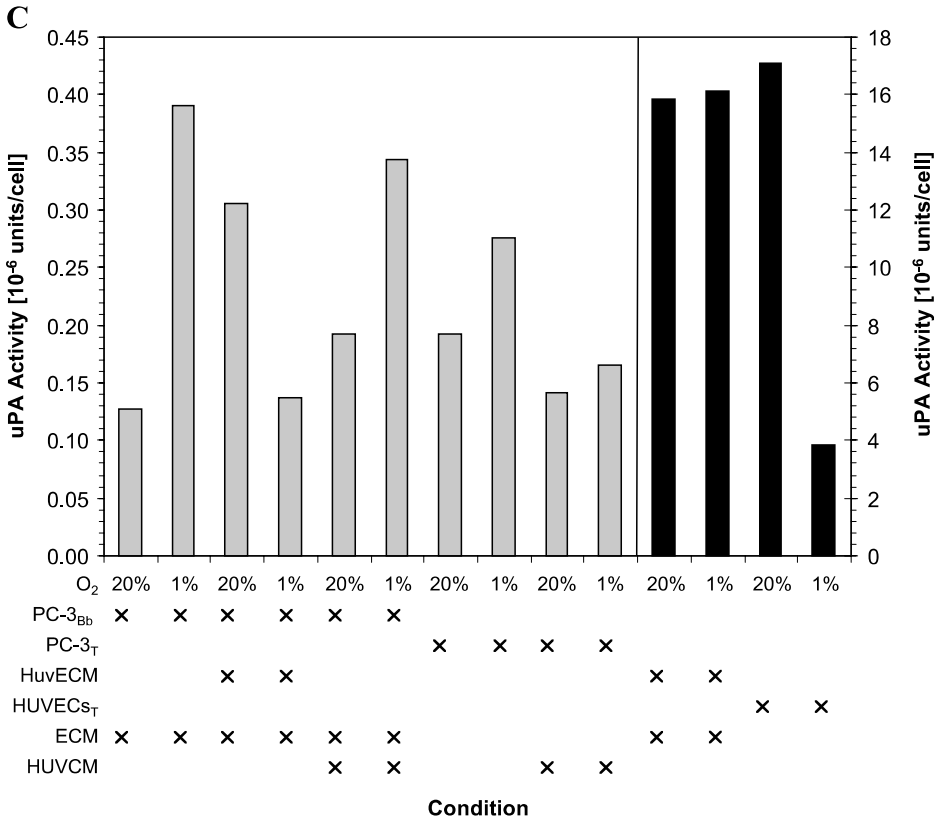

Figure W1. *(continued).*